
**Liquid Crystals**
Publication details, including instructions for authors and subscription information:
http://www.informaworld.com/smpp/title~content=t713926090

# A tilted ferroelectric smectic phase emerging from monomer/polymer mixtures

Alexander Beer[a]; Günter Scherowsky[a]; H. Cackovic[b]; Harry Coles[c]
[a] Inst. f. Org. Chemie, TU Berlin, Berlin, Germany [b] Inst. f. Makromol. Chemie, TU Berlin, Berlin, Germany [c] Physics Department, Liquid Crystal Group, University of Manchester, Manchester, UK

**To cite this Article** Beer, Alexander , Scherowsky, Günter , Cackovic, H. and Coles, Harry(1996) 'A tilted ferroelectric smectic phase emerging from monomer/polymer mixtures', Liquid Crystals, 21: 2, 209 — 216
**To link to this Article: DOI:** 10.1080/02678299608032825
**URL:** http://dx.doi.org/10.1080/02678299608032825

LIQUID CRYSTALS, 1996, VOL. 21, NO. 2, 209–216

# A tilted ferroelectric smectic phase emerging from monomer/polymer mixtures

by ALEXANDER BEER, GÜNTER SCHEROWSKY*, H. CACKOVIC† and HARRY COLES‡

Inst. f. Org. Chemie, TU Berlin, 10623 Berlin, Germany
†Inst. f. Makromol. Chemie, TU Berlin, 10623 Berlin, Germany
‡Physics Department, Liquid Crystal Group, University of Manchester, Manchester M15 9PL, UK

(*Received 27 September 1995; accepted 22 February 1996*)

Mixtures of a fluorescent liquid crystalline side chain polyacrylate and its corresponding ferroelectric monomer were studied by optical microscopy, DSC, X-ray and electro-optic techniques. For some of these mixtures we surprisingly found the emergence of the ferroelectric $S_X^*$ phase, which is not exhibited by the single components. The crystalline phase of the monomer is completely suppressed by polymer concentrations above 25 per cent. The 50 per cent polymer-containing mixture shows a clear eutectic effect for the tilted phases and allows electro-optic switching close to room temperature, more than 40 K below the melting point of the monomer.



## 1. Introduction

Smectic LC side chain polymers are to a certain extent miscible with low molar mass materials of similar structure [1–4]. However, the emergence of a smectic phase which does not exist in the pure components of such a binary LMM/polymer system has not yet been reported, although this phenomenon was recently detected for mixtures of low molar mass materials [5]. The viscosity and response time of ferroelectric hosts are usually raised in polymer/monomer mixtures [2,6]. On the other hand it was found that doping of low molar mass ferroelectric LCs with polymers improves the mechanical shock characteristics with respect to the undoped material [6]. Diluting a ferroelectric polymer with its own monomer also decreases the viscosity of the ferroelectric polymer [2].

Recently we described the preparation and the physical properties of some fluorescent copolymers which are based on a ferroelectric polyacrylate containing various fluorescent dye comonomers [7]. In one of these copolymers, ferroelectric properties were not found, due to the substitution of the tilted $S_C^*$ phase by the orthogonal $S_A$ phase. We prepared binary mixtures of this copolymer and its corresponding ferroelectric monomer in order to improve the properties of the single components.

*Author for correspondence.

## 2. The materials studied

The structures and phase transitions of the fluorescent copolymer **1** and the saturated monomer **2** are given in figure 1. The copolymer exhibits the orthogonal smectic phases $S_B$ and $S_A$. The low molar mass compound is crystalline at room temperature and shows the phase sequence $Cr/S_C^*/S_A/I$. Binary polymer/monomer mixtures containing 25%, 33%, 50%, 60%, 75% and 90% (w/w, respectively) of the polymer were studied by optical microscopy, DSC, X-ray scattering and electro-optic techniques.

## 3. Physical properties of the mixtures

The miscibility of polymer **1** and the low molar mass ferroelectric **2** is very high due to the similar structures of the two materials and the relatively low molar mass $M_w$ of the polymer (figure 1). In fact, both materials are completely miscible over a wide concentration range. Only at low polymer concentrations was the formation of the crystalline phase of compound **2** observed.

### 3.1. *Optical microscopy results*

The optical textures of the mixtures were investigated using antiparallel rubbed polyimide coated cells. Typical textures of the smectic phases are shown in figures 2–5; all pictures are taken with the 50% mixture. The $S_A$ phase (figure 2) was identified by its smooth fan-shaped texture and its rather low viscosity that allowed reasonably good alignment even for high polymer-containing mixtures. On cooling, the $S_C^*$ phase appears (figure 3)

0267–8292/96 $12·00 

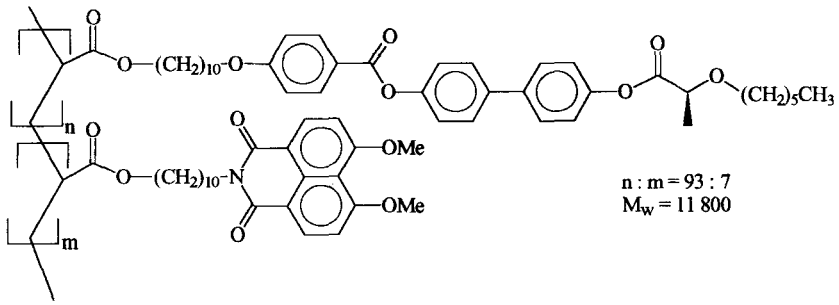


**Copolymer 1 : $S_B$ 75 $S_A$ 120 $S_A$/I 160 I**

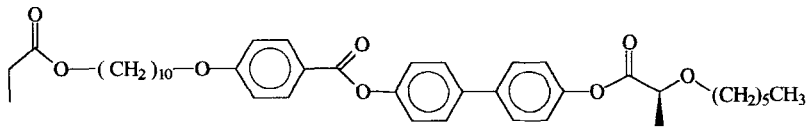

**Saturated Monomer 2 : Cr 71·5 $S_C^*$ 97·0 $S_A$ 110·3 I**

Figure 1. Structures and phase sequences of the copolymer **1** and the monomer **2**.

showing the typical broken fan defect texture. The transition to the underlying $S_X$ phase is indicated by a striped texture with the stripes parallel to the long axis of the fans (figure 4). On further cooling the $S_B$ phase comes in with stripes orthogonal to the fan long axis (figure 5). The $S_B$ phase was identified by comparison with the room temperature $S_B$ phase texture of polymer **1**, which was determined by X-ray diffraction [7].

The transition temperatures of the mixtures on heating, as determined by optical microscopy, are given in the table. Both single components exhibit the $S_A$ phase, as do all the mixtures, as expected. However, the $S_C^*$ phase, which is not shown by the polymer, was found for all the mixtures investigated. The $S_C^*$ phase in mixtures containing 25 to 70% of the polymer is wider in range than for the pure compound **2**. The crystalline phase of compound **2** is completely suppressed in the mixtures with above 25% polymer content, with all mixtures showing the $S_B$ phase at room temperature. At lower polymer concentrations, we found evidence for phase separation due to partial crystallization of the low molar mass component. No further investigations were made on these mixtures.

Surprisingly, we found two enantiotropic phase transitions between the $S_B$ phase and the $S_C^*$ phase for the mixtures of 33 to 90% polymer content, suggesting the existence of a smectic phase $S_X$, which is not exhibited by the single components. For a polymer concentration of 95%, the exact determination of the transition temperatures for the phase sequence $S_B/S_X/S_C^*/S_A$ was impossible due to broad transitions and the rather narrow phase widths of the $S_X$ and $S_C^*$ phases. However, an obvious miscibility gap for the $S_C^*$ phase was not found.

### 3.2. *DSC results*

The DSC traces of the mixtures confirmed the transitions detected by optical microscopy. The only exceptions were the second order $S_C^*$ to $S_A$ phase transitions, due to the generally broader transitions with increasing polymer content. Figure 6 shows the DSC traces on heating for the pure compound **2**, the 25% and the 50% polymer-containing mixtures. The emergence of the $S_X$

Phase sequence and transition temperatures of the investigated mixtures (% w/w) and the single components **1** and **2** on heating, as determined by optical microscopy.

| Material | Phase sequence |
|---|---|
| FLC monomer **2** | Cr 71·5 $S_C^*$ 97·0 $S_A$ 110·3 I |
| mixture 25% polymer | Cr/$S_B$ 62 $S_C^*$ 94·5 $S_A$ 112 $S_A$/I 126·5 I |
| mixture 33% polymer | $S_B$ 48·5 $S_X$ 60 $S_C^*$ 95 $S_A$ 112 $S_A$/I 132 I |
| mixture 50% polymer | $S_B$ 45 $S_X$ 57 $S_C^*$ 93 $S_A$ 114 $S_A$/I 138 I |
| mixture 60% polymer | $S_B$ 48 $S_X$ 66 $S_C^*$ 96·5 $S_A$ 118 $S_A$/I 143 I |
| mixture 75% polymer | $S_B$ 55 $S_X$ 75·5 $S_C^*$ 109·5 $S_A$ 130 $S_A$/I 155 I |
| mixture 90% polymer | $S_B$ 69·5 $S_X$ 80 $S_C^*$ 96 $S_A$ 123 $S_A$/I 156 I |
| copolymer **1** | $S_B$ 75 $S_A$ 120 $S_A$/I 160 I |

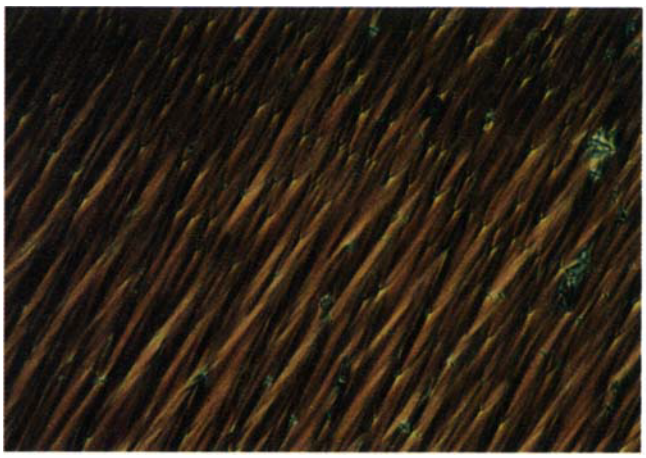

Figure 2. Texture of the $S_A$ phase (50% polymer-containing mixture, 94°C).

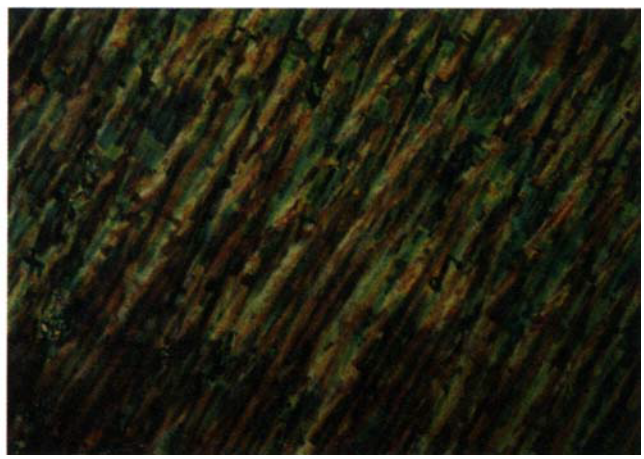

Figure 3. Texture of the $S_C^*$ phase (50% polymer-containing mixture, 69°C).

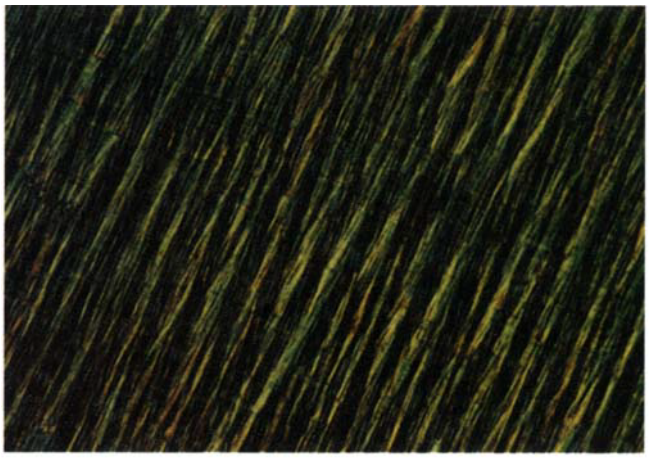

Figure 4. Texture of the $S_X$ phase (50% polymer-containing mixture, 49°C).

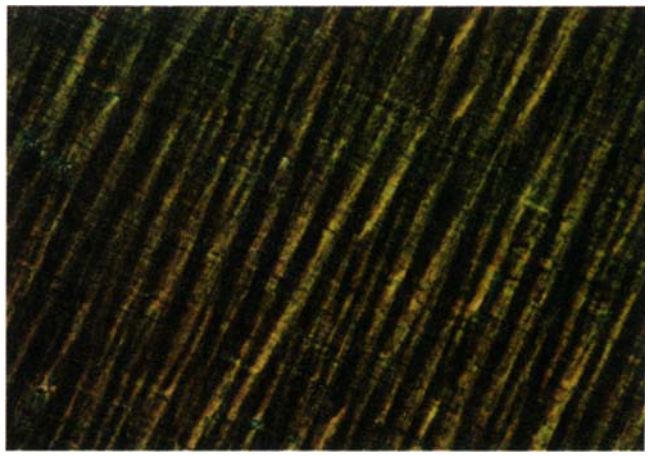

Figure 5. Texture of the $S_B$ phase (50% polymer-containing mixture, 24°C).

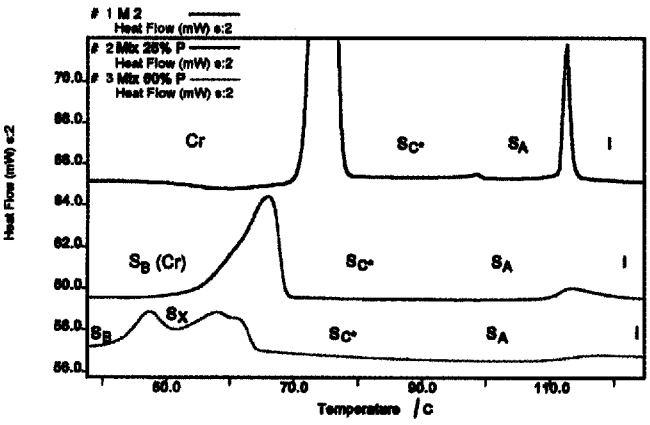


Figure 6. DSC traces of the monomer **2** (black), the 25% (blue) and the 50% (turquoise) polymer-containing mixture on heating (10 K min$^{-1}$).

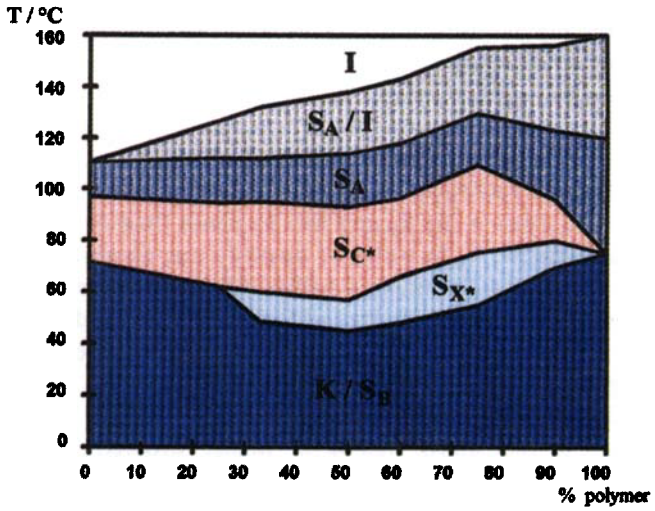


Figure 15. Phase diagram of the binary monomer/polymer system.

phase at 50% polymer concentration can clearly be seen from these traces. However, the transition from the $S_B$ phase to the $S_X$ phase is not yet complete when the $S_X$ to $S_C^*$ phase transition occurs. This is due to the heating rate (10 K $min^{-1}$) and the rather broad phase transitions.

### 3.3. *X-ray results*

X-ray investigations were carried out to learn about the nature of the $S_X$ phase. Figure 7 shows typical X-ray diffraction patterns of aligned samples of the $S_B$ phase, the $S_X$ phase and the $S_C^*$ phase. The pattern of the $S_B$ phase is rather typical. The sharp wide angle reflections show the higher ordering of the molecules within the layers. The small angle reflections caused by the layers are orthogonal to the wide angle signals, proving that the layers are orthogonal to the long axis of the molecules. Within the $S_B$ phase, the layer thickness is constant (figure 8, values taken from the 60% polymer mixture) and matches the length of an extended molecule of compound **2** of approximately 48 Å (calculated using a Dreiding model).

The patterns of the $S_X$ phase and the $S_C^*$ phase differ from typical text book pictures. In the $S_X$ phase the wide angle reflections are rather sharp (figure 7). Small angle reflections appear up to the third order and are slightly tilted with respect to the wide angle signals, indicating that the $S_X$ phase could be a tilted smectic phase. The layer thickness, calculated from the first order short angle reflections, shows a temperature-dependence as it increases with decreasing temperature in the $S_X$ phase (figure 8).

The pattern of the $S_C^*$ phase looks rather like that which would be expected for an $S_A$ phase. However, the layer thickness clearly shows the typical temperature dependence within the $S_C^*$ phase (figure 8). In the $S_A$ phase the layer thickness was found to be independent of the temperature, but smaller than the expected value of 48 Å, indicating a non-extended conformation of the molecules in this phase.

To get information about the molecular ordering within the smectic phases, we took a closer look at the wide angle reflections. Even at first sight these reflections look sharper in the $S_B$ and the $S_X$ phase than in the $S_C^*$ phase (figure 7). In order to quantify our observations, we calculated the integral width (IW) of these signals, which we define as the area of the intensity peak divided by its height (figure 9). For lower ordered phases, one expects higher values of the integral width due to the wider distribution of the molecules within the layers, whereas the sharp signals of higher ordered phases should give lower values. Figure 10 shows a plot of IW versus the temperature for the 60% polymer-containing mixture. The curve shape clearly allows the distinction between lower and higher ordered phases with a turning

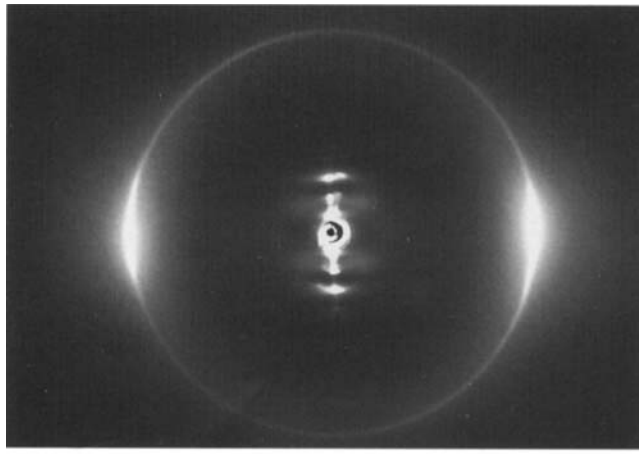

(*a*)

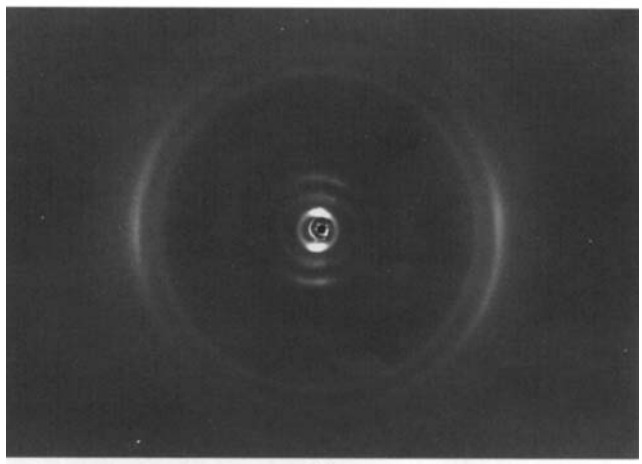

(*b*)

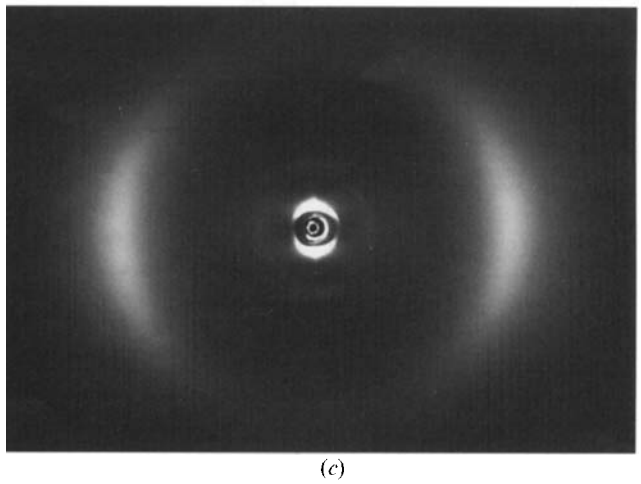

(*c*)

Figure 7. Typical X-ray diffraction patterns taken with the 60% polymer-containing mixture; (*a*) $S_B$ phase at 24°C, (*b*) $S_X$ phase at 50°C and (*c*) $S_C^*$ phase at 70°C.

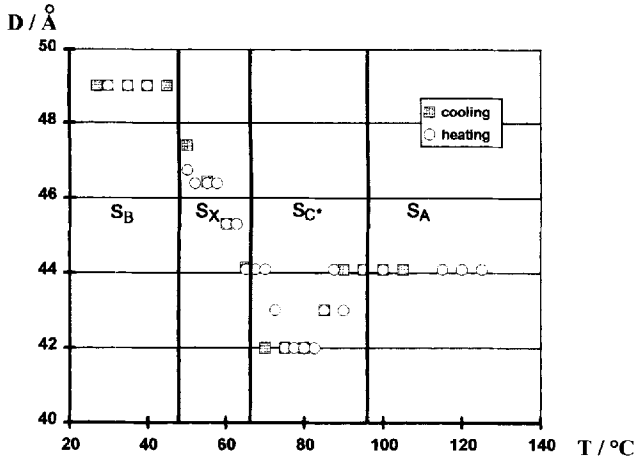


Figure 8. X-ray determined layer thickness ($D$) versus temperature for the 60% polymer-containing mixture; values calculated from the first order short angle reflections.

$$\text{Integral width} = \frac{\textit{peak area}}{\textit{peak height}}$$

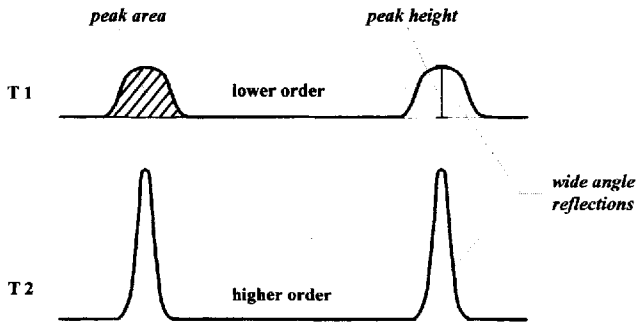


Figure 9. Schematic of the determination of the integral width (IW) from the X-ray wide angle reflections.

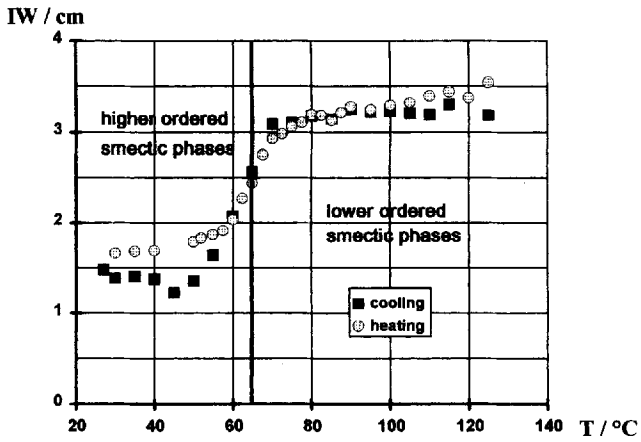


Figure 10. Integral width versus temperature (60% polymer-containing mixture).

point at ~65°C (on heating) due to the $S_X$ to $S_C^*$ phase transition. This value corresponds quite well with the transition temperature determined by optical microscopy as 66°C. The $S_X$ phase is therefore of higher order than the $S_C^*$ phase.

### 3.4. *Electro-optic measurements*

Our electro-optic measurements include the evaluation of the apparent tilt angle ($\theta$), the spontaneous polarization ($P_s$) and the optical response time ($\tau$). The optical tilt angles were measured with low frequency rectangular waveform fields (typically 0·1 Hz) and the values extrapolated to zero field. The $P_s$ values were calculated from the current signals (current pulse technique) using triangular waveform fields. The measured optical response time we defined as the time for a 10 to 90 per cent change in transmission with an applied rectangular waveform field.

All mixtures investigated, and the saturated monomer **2**, show electroclinic switching in the $S_A$ and $S_B$ phase and bistable ferroelectric switching in the $S_C^*$ phase. Additionally we found ferroelectric switching in the $S_X$ phase for all mixtures exhibiting that phase. We take that, along with the X-ray results, as proof that the $S_X$ phase is actually a chiral tilted smectic phase and will hereafter refer to it as the $S_X^*$ phase.

Figures 11 to 14 display the tilt angles, spontaneous polarization values and response times, respectively, of the saturated monomer **2** and the 25%, 50% and 75% polymer-containing mixtures. All compounds show the typical increase of the tilt angle with decreasing temperature within the $S_C^*$ phase (figure 11). The monomer shows the highest tilt values (up to 30°), whereas the values decrease with increasing polymer content from

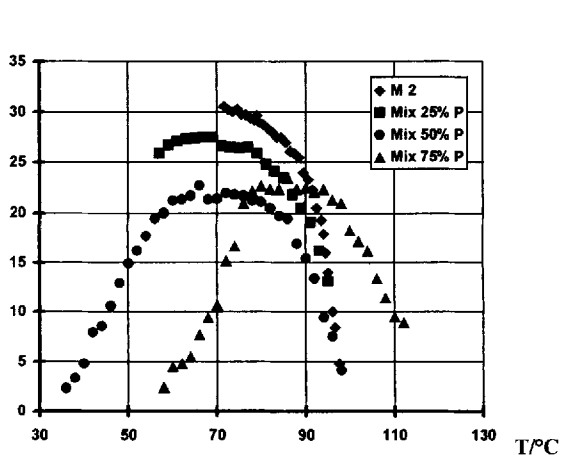


Figure 11. Apparent tilt angles versus temperature for the monomer **2** (diamonds), the 25% polymer-containing mixture (squares), the 50% mixture (circles) and the mixture containing 75% polymer (triangles).

the 25% to the 50% polymer-containing mixture. The tilt angle curves of the 50% and the 75% mixtures are almost equally plateaued and are similar in shape for the $S_C^*$ and the $S_X^*$ phase. Both mixtures show a decreasing tilt angle with decreasing temperature in the $S_X^*$ phase indicating an increasing layer thickness during the approach to the $S_B$ phase. Those results are consistent with the X-ray results on the 60% polymer mixture (see above).

The spontaneous polarization of the monomer shows a steep increase with decreasing temperature in the $S_C^*$ phase (figure 12). A maximum value of 120 nC cm$^{-2}$ was measured in the supercooled $S_C^*$ phase at 58°C. The mixtures exhibit significantly lower $P_s$ values with increasing polymer concentrations. This is rather remarkable, as the chirality of the system undergoes a very small change, from 100% chiral material (monomer **2**) to ~94% chirality (75% polymer mixture). Comparison of the $P_s$ values in the $S_C^*$ phase indicates a linear dependence of the spontaneous polarization on the polymer concentration at several reduced temperatures (figure 13). An extrapolation of the isotherms to 100% polymer content suggests values of 20 to 30 nC cm$^{-2}$ for copolymer **1** in a virtual $S_C^*$ phase. The spontaneous polarization in the $S_X^*$ phase of the 50% and 75% polymer mixtures decreases with decreasing temperature, similarly to the tilt angle. This suggests strong $P$–$\Theta$ coupling.

The spontaneous polarization of the 95% polymer-containing mixture was measured in order to prove the lack of a miscibility gap between the $S_C^*$ phase of the monomer and the $S_A$ phase of the polymer. Small $P_s$ peaks were detected between 73°C and 82°C with a maximum around 77°C. As the peaks were rather broad, the measurements were not particularly accurate; however the $P_s$ value at 77°C is about 10 to 15 nC cm$^{-2}$, which is in the expected range.

The low molar mass compound **2** shows fast optical response times of 12 µs in the $S_C^*$ phase near the $S_A$ phase with an applied field as low as 2·3 V µm$^{-1}$. The response time increases with decreasing temperature to 1000 µs in the supercooled $S_C^*$ phase.

The response time measurements on all mixtures were carried out at 4·3 V µm$^{-1}$ due to the higher threshold voltage of the high polymer-content mixtures. Figure 14 illustrates the strong effect of the polymer on the response times of the mixtures due to the increased

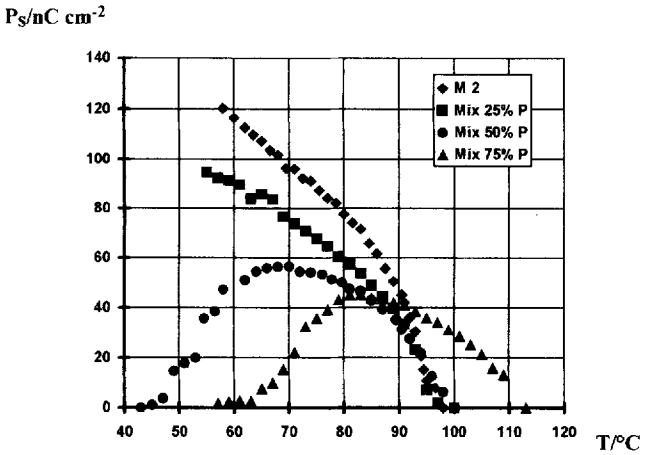


Figure 12. Spontaneous polarization values versus temperature for the monomer **2** (diamonds), the 25% polymer-containing mixture (squares), the 50% mixture (circles) and the mixture containing 75% polymer (triangles).

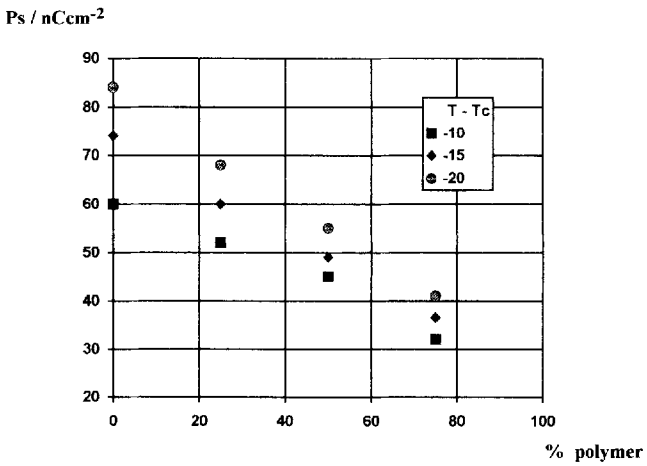


Figure 13. Spontaneous polarization values versus polymer concentration at different reduced temperatures ($T$–$T_c$, $T$ is the actual temperature, $T_c$ is the $S_C^*$ to $S_A$ phase transition temperature).

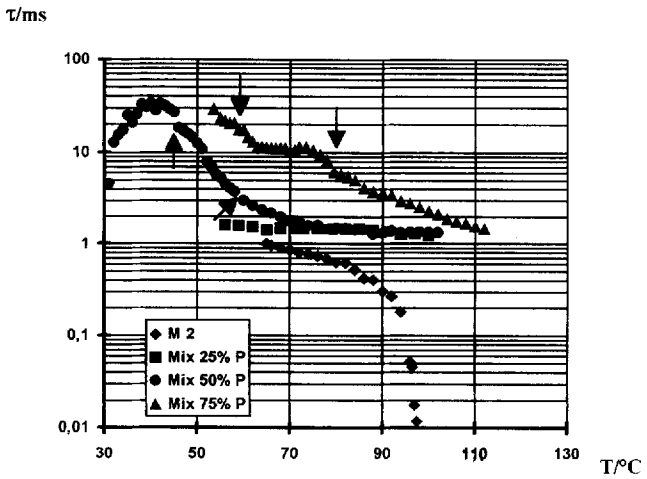


Figure 14. Response times (10–90%) versus temperature for the monomer **2** (diamonds), the 25% polymer-containing mixture (squares), the 50% mixture (circles) and the mixture containing 75% polymer (triangles).

viscosity. Even at higher temperatures, close to the $S_A$ phase transition, the switching time of the mixtures is above 1 ms. This is emphasized even more by the fact that the y-axis of the graph is logarithmic and that the response time of the monomer would be even shorter at 4·3 V $\mu m^{-1}$. However, the 50% polymer-containing mixture can still be switched electroclinically at 30°C in the $S_B$ phase, whereas the single components **1** and **2** are either glassy or crystalline, respectively.

The response time data give further evidence for the $S_C^*$ to $S_X^*$ and $S_X^*$ to $S_B$ phase transitions as can be seen in figure 14. The curves of the 50% and 75% polymer-containing mixtures exhibit discontinuities due to the corresponding phase transitions (indicated by arrows).

## 4. The nature of the $S_X^*$ phase

Optical microscopy and DSC results have proven the existence of the $S_X^*$ phase between the $S_C^*$ phase and the $S_B$ phase. Considering the X ray and electro-optic measurements we can now speculate about the nature of this phase. Ferroelectric switching was found in this phase and the spontaneous polarization was measured; therefore the $S_X^*$ phase is obviously a chiral tilted smectic phase. According to our X-ray data the $S_X^*$ phase is of higher order than the $S_C^*$ phase. All this information leads us to the proposal that the $S_X^*$ phase is either an $S_F^*$ phase or an $S_I^*$ phase. However, one would expect both of these phases to exhibit $P_s$ values and tilt angles higher than those in the $S_C^*$ phase. The spontaneous polarization and tilt angles should also increase with decreasing temperature as they do in the $S_C^*$ phase. We believe that the unusual behaviour of decreasing tilt angles and $P_s$ values with decreasing temperature in the $S_X^*$ phase is caused by the underlying orthogonal $S_B$ phase. As already mentioned above, the transition ranges of the high polymer-containing mixtures are rather broad. Our DSC traces show that the peaks due to the $S_B$ to $S_X^*$ and the $S_X^*$ to $S_C^*$ phase transitions overlap. Therefore the $S_B$ phase has quite a strong influence on the $S_X^*$ phase. This influence increases with decreasing temperature, forcing the molecules in the $S_X^*$ phase to take a more upright position in the layers. Thus the layer thickness increases (see X-ray results) and both the tilt angle and the spontaneous polarization decrease although the mixtures are still in the $S_X^*$ phase.

## 5. Phase diagram

The phase diagram of the binary polymer/monomer system is shown in figure 15. Although it contains the data for only eight different concentrations, it gives a good survey of our binary system. The $S_A$ phase and the biphasic region of the $S_A$ and isotropic phase are given in different colours. The higher ordered $S_B$ phase and the crystalline phase are in one colour, as the miscibility gap could not exactly be determined.

The graph illustrates that with increasing polymer content, the biphasic or clearing temperature range becomes rather broad. The beginning of the clearing range, however, as well as the $S_C^*$ to $S_A$ phase transition are apparently dominated by the low molar mass compound up to a polymer concentration of 50%. From zero to 50% polymer concentration the $S_C^*$ to $S_A$ phase transition temperature decreases slightly by 4 K, while the $S_A$ to $S_A$/I transition slightly increases by 4 K. In the same concentration range, the crystalline or higher ordered phase to $S_C^*$ phase transition shows eutectic behaviour, falling from 71·5°C in the monomer to 57°C in the 1 : 1 mixture. Extrapolation of these transition temperatures to the 100% polymer axis suggests a phase transition temperature of 40 to 50°C for the virtual $S_C^*$ phase of the polymer.

The $S_X^*$ phase does not appear in the monomer or the low polymer concentration mixtures, where the crystalline or $S_B$ phase dominates the lower temperature range. With decreasing melting points, however the $S_X^*$ phase emerges between the $S_B$ and $S_C^*$ phase. The $S_X^*$ phase is most stable at polymer concentrations from 50 to 75%. The width of both tilted phases decreases with increasing polymer concentration above 75% polymer content. Above 90% polymer concentration the tilted phases become rather narrow. However, a miscibility gap between the $S_C^*$ phase of the monomer and the $S_A$ phase of the polymer was not found up to 95% polymer concentration.

## 6. Conclusions

The miscibility of the copolymer **1** and the corresponding ferroelectric monomer **2** was found to be very high. No obvious miscibility gap was detected for the $S_C^*$ phase of the monomer, which appeared in all the investigated mixtures up to 95% polymer concentration. It is not clear whether this means a violation of the miscibility rule [8], as mixtures of higher polymer content could not be investigated.

Although we referred to our mixtures as binary monomer/polymer systems, the polymer is not truly a single component. It consists of a distribution of molecules with different main chain lengths with an average degree of polymerization of 18 units (determined by GPC [7]). It may also contain oligomers of less than 10 monomer units, therefore the excellent miscibility with its corresponding monomer is not really surprising.

Surprising is however the emergence of the higher ordered tilted $S_X^*$ phase from some of our mixtures. Obviously the suppressed crystallization and glass transition of these mixtures allows an additional smectic phase to appear between the $S_B$ and the $S_C^*$ phase. From

our experimental results we suggest that the $S_X^*$ phase is either $S_F^*$ or $S_I^*$.

Our monomer/polymer mixtures show eutectic behaviour for the tilted phases. The 50% polymer-containing mixture shows ferroelectric switching between 45°C and 93°C and exhibits electroclinic switching behaviour down to ~30°C, which is more than 40 K below the melting point of monomer **2**.

## 7. Instrumental

X-ray measurements: X-ray generator ISI-DEBYEFLEX 2002/X-ray valve SF 60/monochromator 151 (Huber). DSC: Perkin-Elmer DSC 7/Indium calibration. Optical microscopy: polarizing microscope Jenapol/hotstage Linkam THM 600 with TMS 90. Electro-optical measurements: ITO test cells parallel or antiparallel rubbed PI/wave generator Phillips PM 5134/amplifier Krohn-Hite 7500/oscilloscope Gould 1602 with wave form processor/photodiode RS Components BPW 21.

## References

[1] SCHEROWSKY, G., GRÜNEBERG, K., and KÜHNPAST, K., 1991, *Ferroelectrics*, **122,** 159.
[2] (*a*) BÖMELBURG, J., 1993, PhD thesis, TU Berlin; (*b*) BÖMELBURG, J., HEPPKE, G., and HOLLIDT, J., 1992, *Polym. Adv. Technol.*, **3,** 237.
[3] TULI, P., and COLES, H. J., 1993, *Liq. Cryst.*, **14,** 1087.
[4] IDO, M., TANAKA, K., HACHIYA, S., and KAWASAKI, K., 1993, *Ferroelectrics*, **148,** 223.
[5] BENNEMAN, D., HEPPKE, G., LÖTZSCH, D., SHARMA, N. K., NEUNDORF, M., and DIELE, S., 1994, 23rd Freiburger Arbeitstagung Flüsigkristalle, Freiburg, Fraunhofer Institut für Angervandte Festkorperphysik, Germany.
[6] LESTER, G., COLES, H. J., MURYAMA, A., and ISHIKAWA, M., 1993, *Ferroelectrics*, **148,** 389.
[7] BEER, A., SCHEROWSKY, G., OWEN, H., and COLES, H. J., 1995 *Liq. Cryst.*, **19,** 565.
[8] SACKMANN, H., and DEMUS, D., 1966, *Mol. Cryst.*, **2,** 81.